Optica Applicata, Vol. XLVII, No. 1, 2017
DOI: 10.5277/oa170108

Abnormal phase removing method in phase measuring profilometry

XINGFEN XU, YIPING CAO*, CHENG CHEN, SENPENG CAO, KUANG PENG

Department of Opto-electronics, Sichuan University, Chengdu, 610065, China

*Corresponding author: ypcao@scu.edu.cn

An abnormal phase removing method in phase measuring profilometry is proposed. In the five equal shifting phase steps algorithm, the shifting phase might be extracted from the deformed patterns captured by CCD camera. But there may be some errors introduced by a digital fringe projector and CCD camera in these deformed patterns. The impurity of the deformed patterns may lead to four classes of abnormalities when extracting the shifting phase. These abnormalities may cause the wrong shifting phase extraction by which the reconstructed object might be misshapen or anamorphic, or even in failure. By this proposed method, the above abnormalities can be removed, and the shifting phase can be auto-extracted precisely from the impure deformed patterns without knowing its value. Experimental results verify the feasibility and effectiveness of the proposed method.

Keywords: information optics, phase measuring profilometry, phase shifting algorithm, phase error, phase auto-extracting.

1. Introduction

With the rapid development of industrialization, the high measurement accuracy of phase-measuring profilometry (PMP) [1–3] makes it useful for various applications, such as product inspection, computer vision, reverse engineering, virtual reality, medical diagnostics and so on [4–8]. In PMP, N ($N \geq 3$) fringe patterns are recorded by CCD camera and the phase distribution can be calculated. The height distribution of the object can be reconstructed by the phase to height mapping [9–11]. However, the phase steps must be strictly controlled by a phase shifter and the shifting phase Φ_0 must be $2\pi/N$ between each adjacent shifting step, which is difficult to operate [12]. In 1997, STOILOV and DRAGOSTINOV proposed the five equal shifting phase steps algorithm (FESPSA) [13], which only requires the shifting phase between each adjacent shifting step equivalent and the total amount of shifting phases need not to be integer multiples of 2π. It is possible to obtain the phase information of the object accurately with FESPSA.

However, the shifting phase Φ_0 excessively depends on the intensity of the captured deformed patterns $I_n(x, y)$. But the digitized errors, random noises from ambient light,

etc., are inevitably brought into $I_n(x, y)$ during the process of capturing. Then the captured $I_n(x, y)$ may bring an error to the shifting phase Φ_0 calculation. It is especially worth noting that, during the process of phase demodulation, $I_n(x, y)$ is involved in the operations of calculating the square root as well as subtraction and division both in the numerator and denominator with $\sin(\Phi_0)$. So the operations will bring abnormalities to $\sin(\Phi_0)$ calculation to some extent. For example, a complex number is found in the operation of extracting a square root and the denominator is zero and so on. Because of the abnormalities, the 3D reconstruction can be affected. There are some burrs on the surface of the measured object, and the distortion is also found on the surface of the reconstructed object, or sometimes the object cannot be reconstructed. So an abnormal phase removing method in phase measuring profilometry is proposed. By this method, the abnormalities can be removed, and the shifting phase can be auto-extracted precisely from the impure patterns without knowing its value in advance. The satisfactory reconstruction result can be derived.

2. Basic concepts of PMP

A schematic of the basic measuring system in PMP is illustrated in Fig. 1. When a sinusoidal granting is projected onto a measured object, CCD camera can capture the deformed pattern modulated by the height of the object. According to the FESPSA, if we shift the phase with an arbitrary nonzero Φ_0 one by one for five steps using the phase shifting device, five frames corresponding to the deformed patterns can be captured by CCD camera, which can be written as

$$I_n(x, y) = R(x, y)\left[A(x, y) + B(x, y)\cos(\Phi(x, y) + n\Phi_0)\right], \quad n = 0, 1, 2, 3, 4 \tag{1}$$

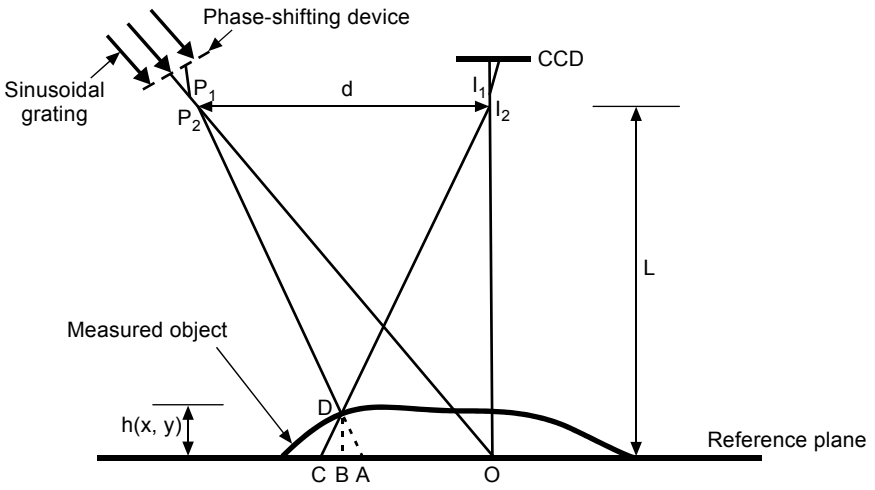

Fig. 1. Phase-measuring profilometry principle.

where $R(x, y)$ is the surface reflectance of the object, $A(x, y)$ is the background light intensity, $B(x, y)$ reflects the fringe contrast, and $\Phi(x, y)$ is the phase information modulated by the height of the object. The phase distribution $\Phi(x, y)$ can be calculated as:

$$\Phi(x, y) = \operatorname{atan}\left\{\frac{2\left[I_1(x, y) - I_3(x, y)\right]}{2I_2(x, y) - I_0(x, y) - I_4(x, y)} \sin(\Phi_0)\right\} \tag{2}$$

$$\sin(\Phi_0) = \sqrt{1 - \left[\frac{I_0(x, y) - I_4(x, y)}{2I_1(x, y) - 2I_3(x, y)}\right]^2} \tag{3}$$

It should be reminded that $\Phi(x, y)$ was mistaken as

$$\Phi(x, y) = \operatorname{atan}\left\{\frac{2\left[I_1(x, y) - I_3(x, y)\right]}{2I_2(x, y) - I_0(x, y) - I_4(x, y)} \frac{1}{\sin(\Phi_0)}\right\} \tag{4}$$

As Equation (2) shows, the atan calculation makes the phase wrapped in the scope from $-\pi$ to π. In fact, the phase distribution is continuous. So the wrapped phase should be unwrapped. Using the diamond phase unwrapping algorithm [14], the wrapped phase $\Phi(x, y)$ can be converted into the continuous phase distribution. This is called the phase unwrapping procedure [15, 16]. It must be pointed out that Eq. (3) shows that the shifting phase Φ_0 depends on the deformed patterns $I_0(x, y)$, $I_1(x, y)$, $I_3(x, y)$ and $I_4(x, y)$. Unfortunately, the digitized errors of a digital light projector or CCD camera, and the disturbance of ambient light could let $I_0(x, y)$, $I_1(x, y)$, $I_3(x, y)$ and $I_4(x, y)$ contain errors, which could cause some unexpected abnormalities in Φ_0 calculation.

3. The abnormal character analyzing

We can see that Φ_0 depends on the intensity of the captured deformed patterns. Grey value acquisition by CCD camera is just an integer between 0 and 255, so digitized errors can be brought in. Secondly, during image acquisition, when the height of the object changes a lot, the phenomenon of distorted stripe dislocation cannot be avoided, and causes the corresponding pixel points of different phase shifting to be mutated. In addition, random noises from ambient light would affect the accuracy of image acquisition. It can be seen from the above analysis that some abnormalities will be obtained when calculating $\sin(\Phi_0)$. For better understanding, a series of numerical simulations have been done. A simulated object "peaks function" with the size 256 × 256 pixels for example is shown in Fig. 2.

When the grating is projected onto the surface of the object and the phase shifting device shifts the phase Φ_0 with $2\pi/5$ for five steps, the corresponding five frames deformed patterns are captured by CCD camera. Figure 2**b** shows one of the deformed

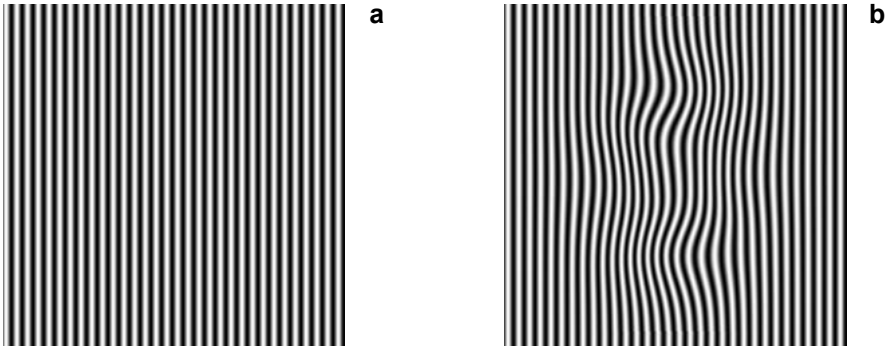

Fig. 2. Projected sinusoidal grating (**a**), and one of deformed patterns (**b**).

patterns. In numerical simulation, $\sin(\Phi_0) = \sin(2\pi/5) = 0.951057$. However, $\sin(\Phi_0)$ will not be a constant according to Eq. (3), and four classes of abnormalities will be found in the result of $\sin(\Phi_0)$.

Firstly, when calculating $I_n(x, y)$ with Eq. (3), we can find $I_1(x, y) = I_3(x, y)$ in some pixel coordinate positions. So the denominator is a zero in Eq. (3). Table 1 reveals 20 positions where $I_1(x, y) = I_3(x, y)$ (called abnormality I). No matter what the amount of $I_0(x, y)$ or $I_4(x, y)$ is, the calculation result of $\sin(\Phi_0)$ is meaningless. These abnormalities will result in the appearance of meaningless phase in their corresponding positions, directly affect phase measurement and phase unwrapping, or even fail to reconstruct the 3D object.

Secondly, there is an extraction s from Eq. (3) as:

$$s = \left[\frac{I_0(x, y) - I_4(x, y)}{2I_1(x, y) - 2I_3(x, y)} \right]^2 \tag{5}$$

An unexpected complex number will be found in the results in some pixel coordinate positions when calculating Eq. (3). If $s > 1$, $\sin(\Phi_0)$ is a complex number. Table 2 shows 20 positions where $s > 1$ (called abnormality II). These abnormalities will result

T a b l e 1. Location for partial abnormalities I.

N	1	2	3	4	5	6	7	8	9	10
x [pixel]	10	14	16	18	117	24	27	40	48	108
y [pixel]	111	167	99	175	129	183	87	195	155	27
$I_1 = I_3$	68	68	107	68	107	68	68	107	68	107
N	11	12	13	14	15	16	17	18	19	20
x [pixel]	88	90	228	115	210	194	192	194	191	184
y [pixel]	74	174	117	111	137	172	142	167	194	142
$I_1 = I_3$	107	68	68	107	68	107	68	107	107	68

T a b l e 2. Location for partial abnormalities II.

N	1	2	3	4	5	6	7	8	9	10
x [pixel]	1	11	11	15	16	18	3	4	4	26
y [pixel]	6	182	190	104	104	86	94	6	22	38
s	1.49	1.25	1.26	1.04	1.08	1.14	1.94	1.94	1.94	1.42
N	11	12	13	14	15	16	17	18	19	20
x [pixel]	95	143	192	206	209	210	212	239	240	238
y [pixel]	64	83	46	222	22	100	181	143	190	103
s	1.13	1.19	1.52	1.53	1.49	1.04	1.09	1.34	1.64	1.86

in the appearance of a complex phase in their corresponding positions and certainly affect phase measurement and phase unwrapping, or even fail to reconstruct the 3D object.

Thirdly, we can also find $I_0(x, y) = I_4(x, y)$ in some pixel coordinate positions when calculating Eq. (3) which will lead $\sin(\Phi_0)$ to be unexpected 1.

In this condition, Φ_0 is $\pi/2$ rather than the pre-set $2\pi/5$. So the calculation of the phase shifting algorithm is seriously incorrect. These abnormalities will lead to the wrong phases when unwrapping the phase and make the reconstruction object misshapen or blurring. As is shown in Table 3, there are 20 positions where $I_0(x, y) = I_4(x, y)$ (called abnormality III).

T a b l e 3. Location for partial abnormalities III.

N	1	2	3	4	5	6	7	8	9	10
x [pixel]	10	12	10	16	21	25	28	29	32	48
y [pixel]	111	107	159	99	179	120	112	187	145	155
$I_0 = I_4$	139	36	139	36	36	139	139	36	139	139
N	11	12	13	14	15	16	17	18	19	20
x [pixel]	70	73	88	90	95	124	146	159	164	171
y [pixel]	115	99	74	174	189	23	192	95	206	202
$I_0 = I_4$	139	36	36	139	36	139	36	139	139	36

Lastly, after excluding the above three classes of abnormalities, the forth abnormality cannot be ignored. There is a division operation in Eq. (3). So when the denominator $2[I_1(x, y) - I_3(x, y)]$ is nonzero but relatively small in number, and the numerator $[I_0(x, y) - I_4(x, y)]$ makes a small change caused by some introduced errors, a major change in division and some transnormal error (called abnormality IV) will be brought in. The 3D reconstruction is seriously anamorphic. Table 4 depicts 20 positions in this condition which lead to transnormal phase errors.

The above analysis is made under the condition of no disturbance of ambient light. We can see that the above four classes of abnormalities are expected to be derived when

T a b l e 4. Location for partial abnormalities IV.

N	1	2	3	4	5	6	7	8	9	10
x [pixel]	12	12	19	19	22	22	23	29	32	34
y [pixel]	49	201	109	149	146	149	154	142	73	110
$\sin(\Phi_0)$	0.98	0.97	0.98	0.99	0.97	0.99	0.98	0.98	0.97	0.99
N	11	12	13	14	15	16	17	18	19	20
x [pixel]	222	225	230	235	237	238	172	172	28	36
y [pixel]	163	180	196	156	76	100	233	249	134	163
$\sin(\Phi_0)$	0.99	0.98	0.99	0.97	0.99	0.98	0.97	0.97	0.99	0.99

unwrapping the phase without the disturbance of ambient light, and they will affect the phase measurement or phase unwrapping seriously. So an abnormal phase removing method in phase measuring profilometry is proposed.

4. Description of the proposed method

After excluding the above four classes of mentioned abnormalities, the rest $\sin(\Phi_0)$ distribution values may be very close to $\sin(2\pi/5)$. However, there are still some small errors in these values caused by the impurity of the captured deformed patterns. Table 5 shows the $\sin(\Phi_0)$ values at and around the (241, 82) pixel coordinate, they are all different but close to $\sin(2\pi/5)$.

T a b l e 5. Values of $\sin(\Phi_0)$ at and around (241, 82) pixel coordinate.

Coordinate	81	82	83
240	0.951058	0.950624	0.949328
241	0.950792	0.950957	0.952041
242	0.951221	0.950763	0.951486

With the proposed method, the phase shifting algorithm can be improved effectually. To some extent, the disturbance of ambient light also can be restrained to a maximum. The detailed abnormal phase removing method is as follows.

1. Calculate $\Delta_1 = I_1(x, y) - I_3(x, y)$. If $\Delta_1 = 0$, $\sin(\Phi_0)$ is masked as a known number far beyond the range of $\sin(\Phi_0)$ such as 100 (as a token of abnormality I).

2. Calculate s. If $s > 1$, $\sin(\Phi_0)$ is masked as another known number far beyond the range of $\sin(\Phi_0)$ such as 200 (as a token of abnormality II).

3. Calculate $I_0(x, y) - I_4(x, y)$. If the result is zero, $\sin(\Phi_0)$ is masked as another known number far beyond the range of $\sin(\Phi_0)$ such as 300 (as a token of abnormality III).

4. Calculate $\sin(\Phi_0)$ with Eq. (3).

5. Scan successively $M \times N$ array of $\sin(\Phi_0)$ distribution, put the $\sin(\Phi_0)$ arranged from 0 to 1 into one-dimensional array A_0, and note the amount K_0 of the dimension.

6. Calculate the mean value $\overline{a_0}$ and root mean squared (RMS) error δ. If δ is more than some pre-set little value ε, it is proved there are some transnormal errors in array A_0. Mark the elements in array A_0 with a known number far beyond its range such as 400 (as a token of abnormality IV).

7. Judge whether there are some tokens of 400 in array A_0. If so, then exclude them and record the number K_0 of the valid elements. Go back to step 6. Otherwise, it is proved the four mentioned abnormalities have been excluded. Calculate the mean value $\overline{a_0}$ of the remaining elements K_0 in array A_0. The elements in array A_0 will be replaced by $\overline{a_0}$ at last.

8. Calculate the phase according to Eq. (2).

In this way, the $\sin(\Phi_0)$ can be extracted precisely and helpful for phase calculation. Take the peaks function as shown in Fig. 2**b**, for example. Though there are so many abnormalities shown in Tables 1–4, the mean value $\overline{a_0}$ is extracted to be 0.951070, very close to $\sin(2\pi/5)$, and the error is less than 1.3×10^{-5}. We can see that the errors brought by the four classes of abnormalities can be removed effectually.

5. Experiment and analysis

The experiments have been implemented to verify the validity of the proposed method. Firstly, a plane with the height of 12.00 mm has been measured. When shifting the phase of the projected grating with an arbitrary nonzero Φ_0 one by one for five steps with the phase shifting device, five frames of the corresponding deformed patterns can be captured by CCD camera. To be convenient for the analysis, here we set the Φ_0 as $2\pi/5$. Figures 3**a** and 3**b** show the wrapped phase with the FESPSA and the proposed method. The height distribution of the measured plane is reconstructed as shown in Fig. 4. Due to the above four classes of abnormalities, Fig. 4**a** shows plenty of blurs or striations on the surface of the reconstructed plane, and Fig. 4**b** shows a better reconstruction result with the proposed method. The corresponding error distributions are shown in Fig. 5. The maximum error in Fig. 5**a** is 2 mm, and the RMS error cannot

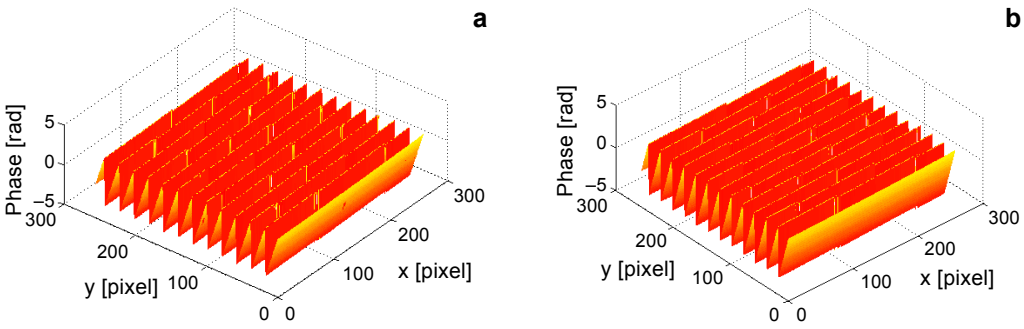

Fig. 3. The wrapped phase with FESPSA (**a**), and with the proposed method (**b**).

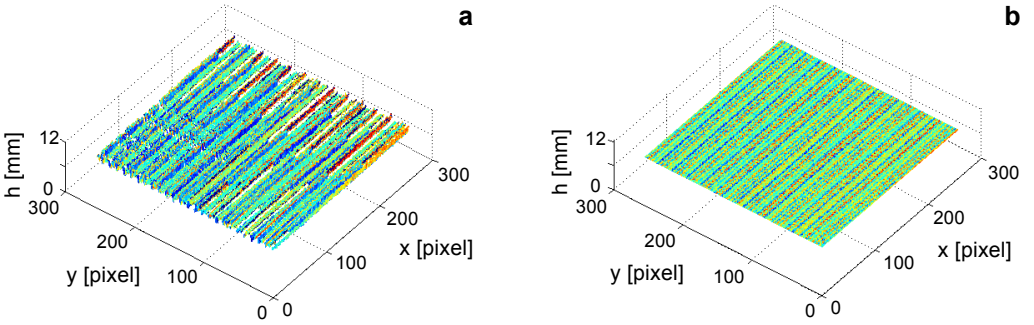

Fig. 4. Reconstruction results with FESPSA (**a**), and with the proposed method (**b**).

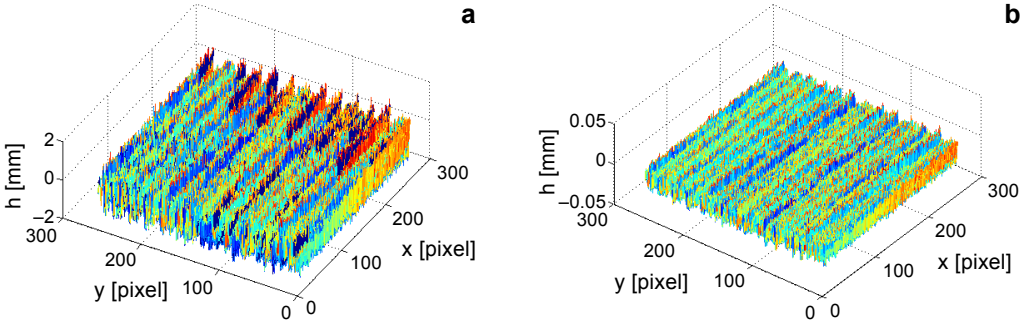

Fig. 5. Error distribution with FESPSA (**a**), and with the proposed method (**b**).

be figured out for there are some meaningless values (labeled in NaN) somewhere. The maximum error in Fig. 5**b** is less than 0.05 mm, and the RMS error in Fig. 5**b** is only less than 0.008 mm, which shows a good measuring precision of the proposed method. To verify the validity of the proposed method with an arbitrary nonzero Φ_0, we make actively Φ_0 produce three different values ($\pi/6, \pi/4, \pi/3$) to measure the above plane. Table 6 shows the results $\overline{a_0}$ with the proposed method. Though there are errors in the mean value $\overline{a_0}$ caused by the impurity of the captured deformed patterns and the capturing errors introduced by the digital light projector or CCD camera, we can see that each $\overline{a_0}$ is very close to its theoretical value. Dealing each $\overline{a_0}$ with the proposed method, the error is not more than 5.2×10^{-4}. Meanwhile, the plane is well reconstructed each time, and the measurement error and its distribution are almost the same

T a b l e 6. Result of $\overline{a_0}$ at different $\sin(\Phi_0)$.

$\sin(\Phi_0)$	$\overline{a_0}$	Error
0.50000	0.50046	0.00046
0.70711	0.70649	0.00052
0.86603	0.86643	0.00040

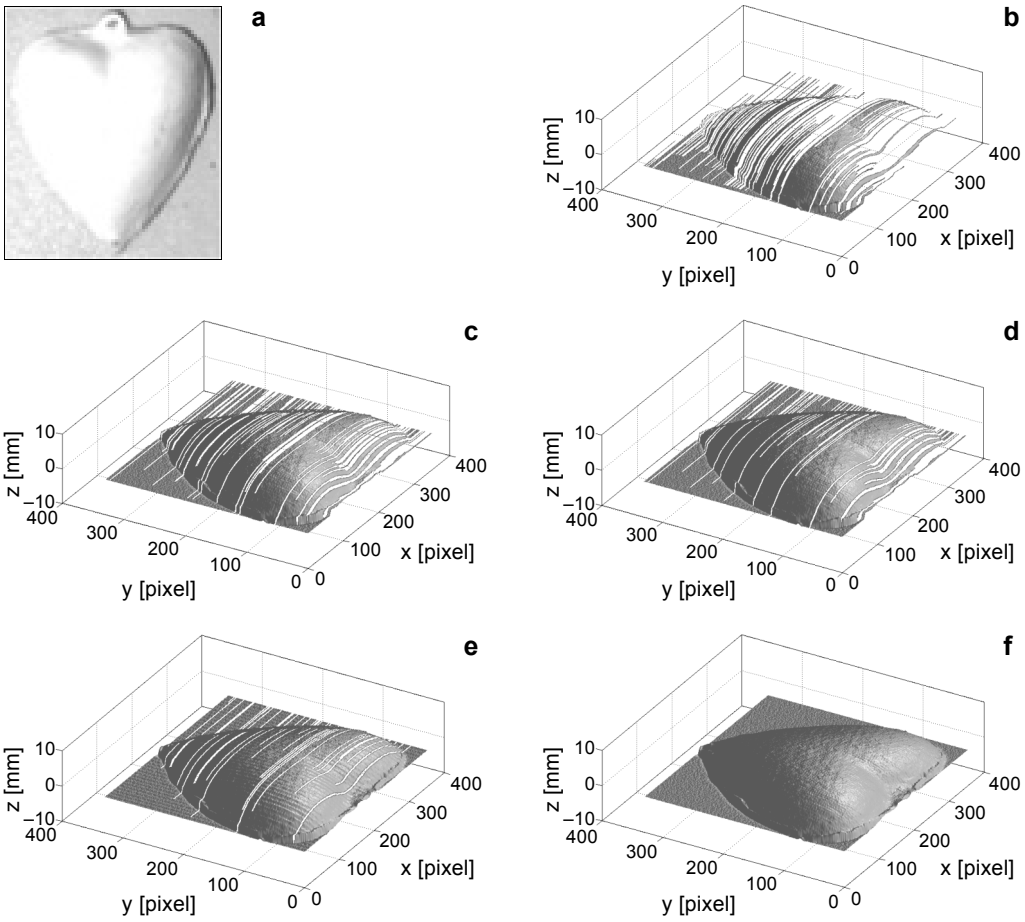

Fig. 6. Experimental data and results. Measured object (**a**), the FESPSA (**b**), exclude abnormality I (**c**), exclude abnormalities I–II (**d**), exclude abnormalities I–III (**e**), and with the proposed method (**f**).

as Fig. 5**b**. So it can be confirmed that the proposed method is valid with an arbitrary nonzero Φ_0.

Secondly, in order to further validate the proposed method feasibility, a heart-shaped object is measured (Fig. 6**a**). Figure 6**b** shows the reconstructed object with FESPSA. The result of the reconstruction is very poor. Figure 6**c** depicts the reconstructed object after excluding the abnormalities I. There is some improvement compared with Fig. 6**b**, but the effect is still poor. After excluding the abnormalities I–II, the reconstruction result is shown in Fig. 6**d**. We can see that the misshapen or anamorphic effect is still serious though it is better than the reconstruction result (Fig. 6**c**). The better reconstruction result is shown in Fig. 6**e** after excluding the abnormalities I–III. But the distortion somewhere is still found in Fig. 6**e**. It is caused mostly by a transnormal er-

ror. After further revisions of the abnormalities IV with the proposed method, the satisfactory reconstruction result can be derived, which is shown in Fig. 6**f**. Therefore, we can confirm that the proposed method is quite feasible and valid.

6. Conclusion

In FESPSA, there may be four classes of abnormalities in the shifting phase Φ_0 distribution which may be caused by some errors introduced by a digital fringe projector, CCD camera and the ambient light. So an abnormal phase removing method in phase measuring profilometry is proposed. In the proposed method, the phase error brought by the four classes of the abnormalities can be removed, and the shifting phase can be auto-extracted precisely from the impure captured deformed patterns without knowing its value. Experimental results show the reliability of the proposed method. The maximum error is less than 0.05 mm and the RMS error is less than 0.008 mm in measuring a plane of 12 mm height.

Acknowledgements – This work was supported by the 863 National Plan Foundation of China under Grant No. 2007AA01Z333 and Special Grand National Project of China under grant No. 2009ZX02204-008.

References

[1] WAN-SONG LI, XIAN-YU SU, *Application of improved phase-measuring profilometry in nonconstant environmental light*, Optical Engineering **40**(3), 2001, pp. 478–485.

[2] SRINIVASAN V., LIU H.C., HALIOUA M., *Automated phase-measuring profilometry of 3-D diffuse objects*, Applied Optics **23**(18), 1984, pp. 3105–3108.

[3] ERYI HU, YUMING HE, YU HUA, *Profile measurement of a moving object using an improved projection grating phase-shifting profilometry*, Optics Communications **282**(15), 2009, pp. 3047–3051.

[4] WU YINGCHUN, CAO YIPING, LU MINGTENG, LI KUN, *An on-line phase measuring profilometry based on modulation*, Optica Applicata **42**(1), 2012, pp. 31–41.

[5] YANSHAN XIAO, YIPING CAO, YINGCHUN WU, *Improved algorithm for phase-to-height mapping in phase measuring profilometry*, Applied Optics **51**(8), 2012, pp. 1149–1155.

[6] BRÄUER-BURCHARDT C., BREITBARTH A., KÜHMSTEDT P., NOTNI G., *High-speed three-dimensional measurements with a fringe projection-based optical sensor*, Optical Engineering **53**(11), 2014, article ID 112213.

[7] SONG ZHANG, *Recent progresses on real-time 3D shape measurement using digital fringe projection techniques*, Optics and Lasers in Engineering **48**(2), 2010, pp. 149–158.

[8] ZHUANG MAO, YIPING CAO, LIJUN ZHONG, SENPENG CAO, *A method for improving the precision of on-line phase measurement profilometry*, Optica Applicata **45**(1), 2015, pp. 51–61.

[9] XINTIAN BIAN, JUNPENG XUE, JU CHENG, BAOWEI JI, HUALING YU, XIANYU SU, WENJING CHEN, *Phase measuring profilometry based on elliptically pattern grating*, Optik – International Journal for Light and Electron Optics **124**(19), 2013, pp. 3924–3928.

[10] SENPENG CAO, YIPING CAO, MINGTENG LU, QICAN ZHANG, *3D shape measurement for moving scenes using an interlaced scanning colour camera*, Journal of Optics **16**(12), 2014, article ID 125411.

[11] CHENG CHEN, YI-PING CAO, LI-JUN ZHONG, KUANG PENG, *An on-line phase measuring profilometry for objects moving with straight-line motion*, Optics Communications **336**, 2015, pp. 301–305.

[12] YEOU-YEN CHENG, WYANT J.C., *Phase shifter calibration in phase-shifting interferometry*, Applied Optics **24**(18), 1985, pp. 3049–3052.
[13] STOILOV G., DRAGOSTINOV T., *Phase-stepping interferometry: five-frame algorithm with an arbitrary step*, Optics and Lasers in Engineering **28**(1), 1997, pp. 61–69.
[14] KUANG PENG, YIPING CAO, YINGCHUN WU, YANSHAN XIAO, *A new pixel matching method using the modulation of shadow areas in online 3D measurement*, Optics and Lasers in Engineering **51**(9), 2013, pp. 1078–1084.
[15] ASUNDI A., ZHOU WENSEN, *Fast phase-unwrapping algorithm based on a gray-scale mask and flood fill*, Applied Optics **37**(23), 1998, pp. 5416–5420.
[16] XIANYU SU, WENJING CHEN, *Reliability-guided phase unwrapping algorithm: a review*, Optics and Lasers in Engineering **42**(3), 2004, pp. 245–261.

Received April 27, 2016
in revised form June 3, 2016